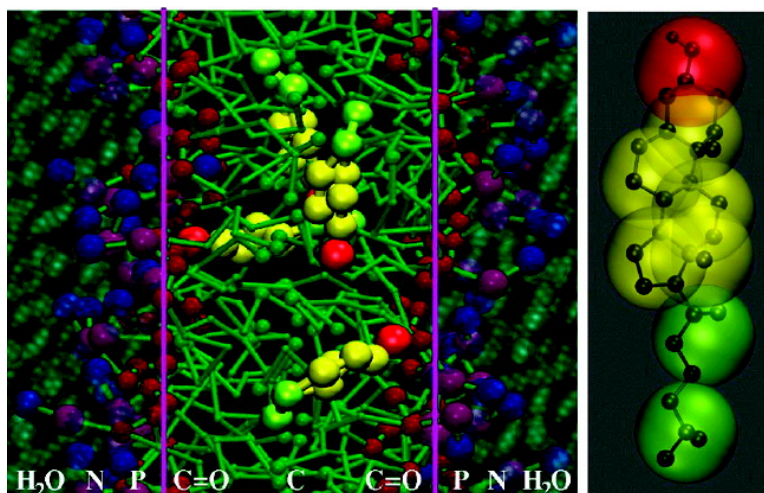


## Cholesterol Shows Preference for the Interior of Polyunsaturated Lipid Membranes

Siewert J. Marrink, Alex H. de Vries, Thad. A. Harroun, John Katsaras, and Stephen R. Wassall

*J. Am. Chem. Soc.*, **2008**, 130 (1), 10-11 • DOI: 10.1021/ja076641c

Downloaded from <http://pubs.acs.org> on February 8, 2009



### More About This Article

Additional resources and features associated with this article are available within the HTML version:

- Supporting Information
- Links to the 12 articles that cite this article, as of the time of this article download
- Access to high resolution figures
- Links to articles and content related to this article
- Copyright permission to reproduce figures and/or text from this article

[View the Full Text HTML](#)

## Cholesterol Shows Preference for the Interior of Polyunsaturated Lipid Membranes

Siewert J. Marrink,<sup>\*,†</sup> Alex H. de Vries,<sup>†</sup> Thad. A. Harroun,<sup>‡</sup> John Katsaras,<sup>‡,§</sup> and Stephen R. Wassall<sup>¶</sup>

*Groningen Biomolecular Sciences and Biotechnology Institute, University of Groningen, Nijenborgh 4, 9747 AG Groningen, The Netherlands, Department of Physics, Brock University, St. Catharines, ON L2S 3A1, Canada, Canadian Neutron Beam Centre, National Research Council, Chalk River, ON K0J 1J0, Canada, and Department of Physics, Indiana University–Purdue University Indianapolis, Indianapolis, Indiana 46202-3273*

Received September 8, 2007; E-mail: s.j.marrink@rug.nl

The physiological importance of polyunsaturated fatty acid (PUFA) is becoming increasingly evident.<sup>1</sup> Sequestration of PUFA-containing phospholipids into cholesterol-depleted membrane domains has been hypothesized to have a role in neurological function and in alleviating a number of health problems.<sup>2</sup> The dislike of highly disordered polyunsaturated chains for the planar, rigid surface of the steroid moiety is thought to be a major driving force for domain formation. Recent neutron scattering experiments<sup>3</sup> showed a striking manifestation of this aversion. Selectively deuterated cholesterol/1,2-diarachidonylphosphatidylcholine (DAPC) samples revealed that the hydroxyl of the sterol resides at the center of the bilayer. This result was interpreted in terms of cholesterol preferentially sequestering inside the membrane and in contrast to its usual position where the hydroxyl group locates near the aqueous interface.

The recently developed MARTINI coarse grained (CG) model<sup>4</sup> is used to simulate the behavior of cholesterol inside lipid bilayers. The MARTINI model unites small groups of atoms into CG beads, allowing simulation times in the microsecond range while practically retaining atomic resolution detail. The model reproduces a variety of structural, dynamic, and thermodynamic properties of lipid membranes on a semiquantitative level. In the current study, molecular dynamics simulations<sup>5</sup> were performed for lipid bilayers with a varying degree of fatty acid unsaturation. The system details were chosen to match the experimental conditions,<sup>3</sup> as closely as possible. Specifically, we modeled 1-palmitoyl-2-oleoyl-PC (POPC, 16:0–18:1 PC), 1-stearoyl-2-arachidonyl-PC (SAPC, 18:0–20:4 PC), and DAPC (20:4–20:4 PC), each containing 10 mol % of cholesterol at a temperature of 300 K. The parameter set for cholesterol was taken from ref 4, and the mapping is shown in Figure 1C. Parameters for the polyunsaturated chains were optimized using results from all-atom simulations.<sup>6</sup> To verify our model, we compared the bilayer thickness and repeat distance for the systems simulated to the experimental data and found good agreement (see Table 1).

Figure 1 shows the neutron scattering density profiles for the DAPC/cholesterol system obtained from our simulations, in comparison to the experimental profile. Figure 1A displays both the total scattering profile and the profile arising from only the deuterated [2,2,3,4,4,6-<sup>2</sup>H<sub>6</sub>] cholesterol moiety. In agreement with the experimental findings, the simulations show a clear presence of the cholesterol head group for the membrane interior. In Figure 1B, a graphical snapshot is presented, showing cholesterol molecules lying between the leaflets, in addition to cholesterols in their usual

orientation. No evidence is found for an upside-down position, an unlikely possibility that could not be ruled out based on the published experimental data. Dimerization of cholesterol molecules embedded inside the bilayer was also not found to be significant. From the relative population densities, the free energy difference between cholesterol in the usual and interior positions can be estimated. Our simulations predict both orientations to be almost equally probable (within  $kT$ ; see Table 1), whereas the experimental data point to a more favorable interior orientation.<sup>7</sup> These quantitative discrepancies we attribute to the approximate nature of the CG model used. Upon increasing the saturation level of the lipid tails (DAPC–SAPC–POPC), the simulations show a drastic shift of the relative population toward the usual orientation, recently confirmed experimentally. In SAPC bilayers, still a small but noticeable fraction of interior cholesterol is observed, while in POPC, cholesterol is almost exclusively found aligned with the phospholipid chains. To discriminate between the effect of unsaturation level and bilayer thickness, simulations were also performed for a dipolyunsaturated lipid with tetracosatetraenoyl chains containing four additional methylenes (DTPC, 24:4–24:4 PC). The relative populations of cholesterol aligned perpendicular and parallel to the bilayer normal remained similar compared to the dipolyunsaturated analogue with 20:4 tails, showing that bilayer thickness is not the main factor when it comes to the orientation of cholesterol in the membrane. Rather, the area per lipid appears to correlate with cholesterol positioning, a prediction that could be tested experimentally.

In Figure 2, the dynamical<sup>8</sup> behavior of cholesterol is analyzed in more detail for each of the three systems. Figure 2A shows the time-dependent orientation of individual cholesterol molecules with respect to the bilayer normal. The histograms of these time series are shown in Figure 2B, and a characteristic flip-flop event is shown in Figure 2C. Some of the properties extracted from these data are summarized in Table 1. Our simulations indicate that the time-dependent behavior of cholesterol depends strongly on the saturation level of the lipids. In the dipolyunsaturated DAPC membrane, cholesterol is undergoing rapid flip-flops between the two monolayers, spending a considerable amount of time in the membrane interior, in line with the neutron scattering data. The flip-flop event is usually triggered by large fluctuations in cholesterol orientation, putting the sterol body almost parallel to the membrane interface. At this point, it becomes favorable for the sterol body to reside in the low-density central part of the membrane's interior, overcoming the energy cost for breaking the hydrogen bonds of the hydroxyl group with the membrane/water interface. Reorientation toward the other interface follows the same steps, but in reverse. The average time between flip-flops in DAPC is 100 ns, corresponding to a

<sup>†</sup> University of Groningen.

<sup>‡</sup> Brock University.

<sup>§</sup> Canadian Neutron Beam Centre.

<sup>¶</sup> Indiana University–Purdue University Indianapolis.

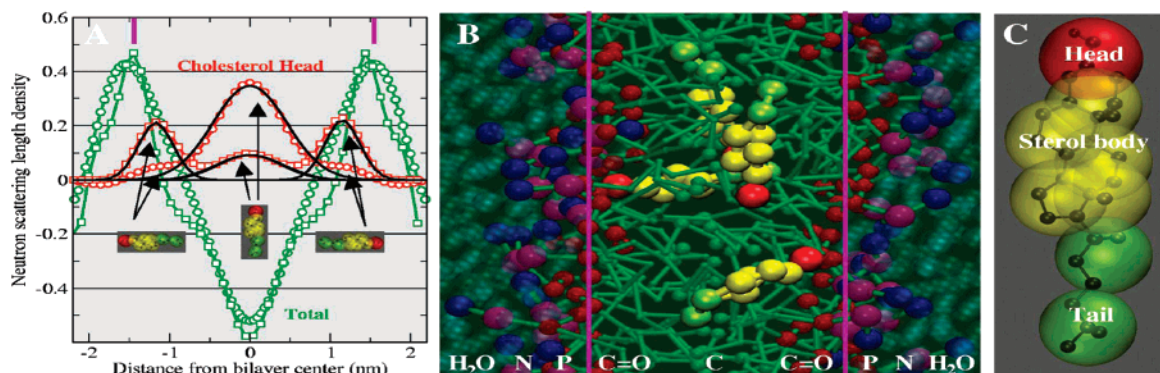


**Figure 1.** (A) Total system neutron scattering profiles (green) and the difference profile between labeled and unlabeled cholesterol head groups (red, multiplied by 5), from simulations (squares) and experiments<sup>3</sup> (circles). Gaussian fits to the individual populations are shown in black. The arrows point to the density maxima, indicating the usual and special orientation of cholesterol. (B) Image illustrating the instantaneous positions of the four cholesterol molecules in a DAPC membrane. The magenta lines correspond to the maxima of the total neutron scattering profile. The lipid tails are shown in green, the glycerol group dark red, phosphate purple, choline blue, and water cyan. (C) The color scheme and mapping to the chemical structure of cholesterol.

**Table 1.** System Properties in Simulations/Experiment

| lipid | $d^a$<br>(nm) | $R^a$<br>(nm) | $A^a$<br>(nm <sup>2</sup> ) | $\theta_{\max}^b$<br>(deg) | $t_{\text{flip}}^c$<br>( $\mu$ s) | $\Delta G^d$<br>(kJ/mol) |
|-------|---------------|---------------|-----------------------------|----------------------------|-----------------------------------|--------------------------|
| POPC  | 3.5/3.65      | 5.6/5.45      | 0.58                        | $18 \pm 16$                | $4.5 \pm 3$                       | 11                       |
| SAPC  | 3.4/3.49      | 5.3/5.29      | 0.68                        | $24 \pm 20$                | $0.5 \pm 0.3$                     | 5                        |
| DAPC  | 2.9/3.06      | 4.6/4.64      | 0.78                        | $30 \pm 22$                | $0.10 \pm 0.05$                   | 2                        |
| DTPC  | 3.3           | 5.0           | 0.78                        | $24 \pm 21$                | $0.15 \pm 0.05$                   | 3                        |

<sup>a</sup> Bilayer thickness ( $d$ ), repeat distance ( $R$ ), and area/lipid ( $A$ ) in simulation/experiment (from scattering profiles<sup>3</sup>). <sup>b</sup> Most probable angle  $\theta_{\max}$   $\pm$  SD of cholesterol with respect to the bilayer normal. <sup>c</sup> Cholesterol flip-flop time  $t_{\text{flip}} \pm$  SD. <sup>d</sup> Free energy difference  $\Delta G$  between standard and interior position of cholesterol. See Supporting Information for more details.

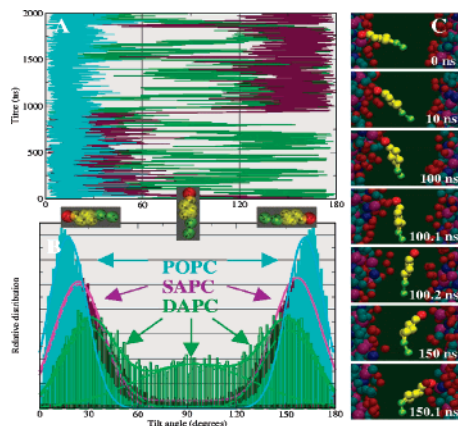


**Figure 2.** Characterization of cholesterol's orientation inside POPC (blue), SAPC (purple), and DAPC (green) membranes. Values of 0 and 180° indicate alignment with the membrane normal in either monolayer; 90° indicates a perpendicular position. (A) Time-dependent orientation for individual cholesterol. (B) Time-averaged distributions with Gaussian fits to the total (solid) and individual (dashed) populations. (C) Time sequence of a cholesterol flip-flop in a DAPC bilayer.

flip-flop rate of  $10^7 \text{ s}^{-1}$ . The residence time in the membrane interior is in the range of 10–100 ns. Similar values are observed for the DTPC bilayer. For SAPC, the flip-flop time increases to 500 ns, and for POPC, it shifts into the microsecond range. This is still fast compared to the rate of flip-flop for phospholipids that, even when greatly enhanced by PUFA,<sup>9</sup> is likely too slow to be observed in the simulations. The distribution of orientation for cholesterol

within the membrane also shows clear differences between the three systems (Figure 2B). Upon increasing saturation, both the most probable (“tilt”) and the average angle relative to the bilayer normal become smaller and the distributions narrower. In other words, unsaturated lipids cause cholesterol to adopt severely tilted orientations, also in its usual position. A larger tilt angle in dipolyunsaturated PC membranes is also a feature of solid-state <sup>2</sup>H NMR experiments.<sup>10</sup> Because the NMR work employed multilamellar dispersions, the axis about which the sterol undergoes axial rotation and with respect to which the tilt angle refers cannot be assigned. The bilayer normal was assumed, an assumption that no longer appears universally applicable.

In conclusion, our CG simulations provide further insight into the interactions of cholesterol with PUFA-containing phospholipids. The aversion between these molecules results in fast flip-flop rates for the sterol and an increased preference of the sterol for the unusual location embedded between the monolayer leaflets.

**Supporting Information Available:** Details about the CG model and the data analysis. Results from all-atom simulations. This material is available free of charge via the Internet at <http://pubs.acs.org>.

## References

- (1) Stillwell, W.; Wassall, S. R. *Chem. Phys. Lipids* **2003**, *126*, 1.
- (2) (a) Mitchell, D. C.; Litman, B. J. *Biophys. J.* **1998**, *74*, 879. (b) Huster, D.; Arnold, K.; Gawrisch, K. *Biochemistry* **1998**, *37*, 17299. (c) Wassall, S. R.; Brzustowicz, M. R.; Shaikh, S. R.; Cherezov, V.; Caffrey, M.; Stillwell, W. *Chem. Phys. Lipids* **2004**, *132*, 79.
- (3) Harroun, T. A.; Katsaras, J.; Wassall, S. R. *Biochemistry* **2006**, *45*, 1227.
- (4) (a) Marrink, S. J.; de Vries, A. H.; Mark, A. E. *J. Phys. Chem. B* **2004**, *108*, 750. (b) Marrink, S. J.; Risselada, H. J.; Yefimov, S.; Tieleman, D. P.; de Vries, A. H. *J. Phys. Chem. B* **2007**, *111*, 7812.
- (5) Simulations were performed using GROMACS: van der Spoel, D.; Lindahl, E.; Hess, B.; Groenhof, G.; Mark, A. E.; Berendsen, H. J. C. *J. Comput. Chem.* **2005**, *26*, 1701.
- (6) Feller, S. E.; Gawrisch, K.; MacKerell, A. D., Jr. *J. Am. Chem. Soc.* **2002**, *124*, 318.
- (7) The experimental profile also shows density for the cholesterol head group at the usual position around  $\pm 1.2$  nm; see arrows in Figure 1A. Due to the limited resolution of the experimental data ( $\sim 1$  nm), it is not clear whether this is realistic or an artifact from the reconstruction procedure.
- (8) An effective time scale is used; see Supporting Information.
- (9) Armstrong, V. T.; Brzustowicz, M. R.; Wassall, S. R.; Jenki, L. J.; Stillwell, W. *Arch. Biochem. Biophys.* **2003**, *414*, 74.
- (10) Brzustowicz, M. R.; Stillwell, W.; Wassall, S. R. *FEBS Lett.* **1999**, *451*, 197.

JA076641C